


A high-resolution projected climate dataset for Vietnam: Construction and preliminary application in assessing future change

Quan Tran-Anh^a, Thanh Ngo-Duc ^{b,*}, Etienne Espagne^c and Long Trinh-Tuan^d

^a Hanoi University of Mining and Geology, Hanoi, Vietnam

^b Department of Space and Applications, University of Science and Technology of Hanoi (USTH), Vietnam Academy of Science and Technology (VAST), Hanoi, Vietnam

^c French Development Agency (AFD), Paris, France

^d Center for Environmental Fluid Dynamics, VNU University of Science, Hanoi, Vietnam

*Corresponding author. E-mail: ngo-duc.thanh@usth.edu.vn

 TN, 0000-0003-1444-7498

ABSTRACT

This study generates a daily temperature and precipitation dataset over Vietnam at a high resolution of 0.1° for the historical period 1980–2005 and the future period 2006–2100 under four representative concentration pathway (RCP) scenarios, namely RCP2.6, RCP4.5, RCP6.0, and RCP8.5. The bias correction (BC) and spatial disaggregation (SD) method is applied to the outputs of 31 global climate models (GCMs) of the Coupled Model Intercomparison Project Phase 5 (CMIP5) to create the new dataset called CMIP5-VN. To guide the BC and SD steps, gridded temperature and precipitation data interpolated from daily observations of 147 and 481 stations respectively are used. Results with the CMIP5-VN show that warming over Vietnam is projected to continue till the end of the 21st century under all four RCPs. The average temperature is projected to increase by 1.3 ± 0.52 °C under RCP2.6 and by 3.85 ± 0.85 °C under RCP8.5 between 2080–2099 and 1986–2005. The future increase is more intense in the northern regions than in the south and higher in summer than in winter. Precipitation is projected to increase by $1.16 \pm 7.1\%$ under RCP2.6 and by $4.41 \pm 9.2\%$ under RCP8.5. In Central Vietnam, there is a consistent rainfall increase in the future rainy season.

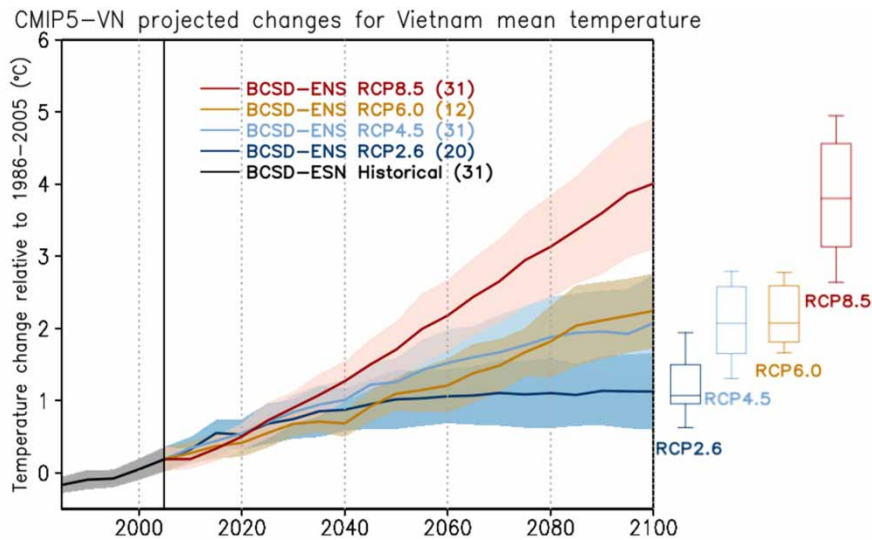
Key words: BCSD, bias correction, climate downscaling, CMIP5, spatial disaggregation, Vietnam

HIGHLIGHTS

- This is the first time a complete set of high-resolution temperature and precipitation data for different scenarios has been created for Vietnam.
- Besides RCP4.5 and RCP8.5, this is the first time the detailed changes under the RCP2.6 and RCP6.0 scenarios in the sub-regions of Vietnam are assessed.
- The warming is more intense in the northern regions than in the south and higher in summer than winter for all RCPs.
- Projected temperature changes relative to the baseline period 1986–2005 based on the newly-created CMIP5-VN data for Vietnam. Five-year moving averages are applied. Colored lines show the ensemble means of the models, and colored shaded areas present the uncertainty ranges (± 1 standard deviation) for each representative concentration pathway (RCP) scenario. The number of models used for each RCP is shown in brackets. Box plots display the occurrence statistics (the ends of the box are the upper and lower quartiles, the horizontal line inside the box marks the median, and the two horizontal lines outside of the box indicate the 10th and 90th percentile values, respectively) for warming levels at the end of the 21st century.

This is an Open Access article distributed under the terms of the Creative Commons Attribution Licence (CC BY-NC-ND 4.0), which permits copying and redistribution for non-commercial purposes with no derivatives, provided the original work is properly cited (<http://creativecommons.org/licenses/by-nc-nd/4.0/>).

GRAPHICAL ABSTRACT



Projected temperature changes relative to the baseline period 1986–2005 based on the newly-created CMIP5–VN data for Vietnam. 5-year moving averages are applied. Colored lines show the ensemble means of the models, and colored shaded areas present the uncertainty ranges (± 1 standard deviation) for each representative concentration pathway (RCP) scenario. The number of models used for each RCP is shown in brackets. Box plots display the occurrence statistics (the ends of the box are the upper and lower quartiles, the horizontal line inside the box marks the median, and the two horizontal lines outside of the box indicate the 10th and 90th percentile values, respectively) for warming levels at the end of the 21st century.

INTRODUCTION

The Sixth Assessment Report (AR6) of the Intergovernmental Panel on Climate Change (IPCC) indicates that the global average surface temperature during 2010–2019 has increased by $\sim 1.09^\circ\text{C}$ compared to 1850–1900 (Arias *et al.* 2021). The warming is projected to be virtually certain in the future at global and regional scales (Arias *et al.* 2021). To assess the impacts of global warming and prepare for response measures, future climate information at different spatial scales, including local and regional ones, is needed (Milly *et al.* 2008; Giorgi & Bi 2009).

The Coupled Model Intercomparison Project (CMIP) is an international experimental protocol coordinated by the World Climate Research Programme (WCRP) for producing and studying the outputs of global climate models (GCMs). Providing the scientific ground for the IPCC Fifth Assessment Report (AR5) (IPCC 2013), the CMIP Phase 5 (CMIP5) provides simulations from GCMs that reflect a joint effort involving many climate research organizations worldwide (Taylor *et al.* 2012). In the CMIP5 project, historical and future climate simulations under different representative concentration pathway (RCP) scenarios were conducted. The RCP scenarios were developed based on the future estimated radiative forcing, covering a period up to the year 2100 or later (van Vuuren *et al.* 2011). There are four RCPs consisting of RCP2.6 (a scenario characterized by a low radiative forcing level), RCP4.5 and RCP6.0 (medium stabilization scenarios), and RCP8.5 (a high radiative forcing scenario). The RCPs represent different pathways upon the projected impacts of land use and emission of greenhouse gases (GHGs). Accordingly, RCP2.6 expresses a low GHG concentration scenario in the future with radiative forcing estimated at 2.6 W/m^2 by 2100, and so forth with the other RCPs (Moss *et al.* 2010).

Though CMIP5 outputs can generally reproduce the major climate indicators at global scales, it is still challenging to directly use them to produce relevant climate information at local to regional scales due to their coarse spatial resolution (typically coarser than 100 km) (Taylor *et al.* 2012; Eyring *et al.* 2016). This raises concerns about adequately using such products as the driving force in other comprehensive environment-socio-economic assessment models to obtain reliable results to support researchers and policymakers in regional planning. Thus, downscaling methods, which transfer data of GCM from a coarse grid resolution into a much higher spatial resolution, should be applied for limited-area domains.

There are two popular downscaling approaches: dynamical and statistical. For dynamical downscaling, higher-spatial resolution models, which are often known as regional climate models (RCMs), are used. Initial and lateral boundary conditions of an RCM are commonly provided by large-scale GCM products, consisting of wind, temperature, and moisture fields. Although dynamical downscaling has the advantage of well representing the local-scale feedback and dynamical processes (Seaby *et al.* 2013; Giorgi & Gutowski 2015; Tangang *et al.* 2020), it is an extremely computationally demanding method; thus, its application for downscaling multiple GCMs and scenarios is limited. For statistical downscaling, it is conducted based on empirical, spatial, and temporal relationships between large-scale and local-scale climate variables (Murphy 1999; Fowler Blenkinsop & Tebaldi 2007). These relationships are assumed to be unchanged with time; thus, they can be used to project future conditions. The primary advantage of statistical downscaling is that it is computationally inexpensive and much faster than dynamical downscaling so that it can be easily applied to generate high-resolution simulations with multiple GCMs. Additionally, statistical downscaling can provide climate information at any specific resolution, so its results can be directly used in climate change impact assessments.

Previous studies showed the skillful performance of different statistical methods (Salathé 2003; Widmann *et al.* 2003; Maurer & Hidalgo 2008; Noël *et al.* 2021). Among those methods, the bias correction and spatial disaggregation (BCSD) approach is reliable and effective for downscaling temperature and precipitation data (Wood 2002; Wood *et al.* 2004). The BCSD has been extensively adopted in various studies in many parts of the world, e.g., in the United States (Rasmussen *et al.* 2016), South Korea (Eum *et al.* 2017), China (Xu & Wang 2019), and at the global scale (Zhang *et al.* 2019).

Located in the tropical region in Southeast Asia, with a long coastline of about 3260 km and an estimated total area of 329,560 km², Vietnam is one of the countries heavily affected by climate change (MONRE 2009). Therefore, to prepare for short- and long-term action plans to cope with climate change, it is important for Vietnam to establish reliable climate change information. As a result, Vietnam's sea-level rise and climate change (SLRCC) scenarios were released in 2009 and 2012 (MONRE 2009, 2012) and followed up with the updated versions in 2016 and 2021 (MONRE 2016, 2021). In the latest SLRCC scenario, outputs of 16 dynamical downscaling experiments based on five different RCMs and 10 driving GCMs for two scenarios, RCP4.5 and 8.5, were analyzed. It should be noted that the accuracy of an RCM simulation depends on the quality of its driving GCM (Déqué *et al.* 2012; Diaconescu & Laprise 2013; Tamara *et al.* 2019); thus, using several GCMs for limited downscaling cases may result in inconsistent future projections. Under the framework of the Coordinated Regional Climate Downscaling Experiment-Southeast Asia (CORDEX-SEA), different dynamical downscaling simulations using seven different RCMs were conducted (Trinh-Tuan *et al.* 2019; Tangang *et al.* 2020; Nguyen-Thuy *et al.* 2021), providing additional projected climate information for Vietnam. However, the number of driving GCMs (11) and scenarios (two) used in CORDEX-SEA is still limited, leading to the possibility that their climate projections might fall outside what would happen in the future. Therefore, our present study is a primary attempt to develop a new comprehensive and high-resolution dataset over Vietnam from a large number of CMIP5 GCMs. The newly-built data, hereafter called CMIP5-VN, consisting of daily mean, maximum, and minimum temperature, and precipitation, are created using the BCSD downscaling method based on a total of 31 CMIP5 GCMs and four RCPs. The new CMIP5-VN dataset is expected to supplement the existing climate change data in Vietnam that were previously obtained by the dynamical downscaling method. In the Results and Discussion section, we also present an application of the CMIP5-VN in assessing future changes in temperature and rainfall over the different climatic sub-regions of Vietnam.

DATA AND METHODS

Study domain

Vietnam has a diverse topography and specific location in the eastern part of the Indochina Peninsula. Mountainous areas cover three-quarters of Vietnam's territory while lowland areas are mainly found in the eastern coastal regions and the two largest deltas of Vietnam, i.e., the Red River and the Mekong deltas. Based on radiation, temperature, and rainfall criteria, Vietnam's climate has been divided into seven climatic sub-regions, including (1) the Northwest (denoted as R1), (2) the Northeast (denoted as R2), (3) the Red River Delta (denoted as R3), (4) the North Central (denoted as R4), (5) the South Central (denoted as R5), (6) the Central Highland (denoted as R6), and (7) the South region (denoted as R7) (Nguyen & Nguyen 2004; Phan *et al.* 2009) (Figure 1). In the north (south) climate domain of Vietnam, which includes four (three) sub-regions R1–R4 (R5–R7), the annual temperature range is larger (smaller) than 9 °C, the total annual irradiation is smaller (larger) than 140 kcal/cm²/year, and the annual sunshine hours is less (more) than 2000 h. The period of the rainy season varies among

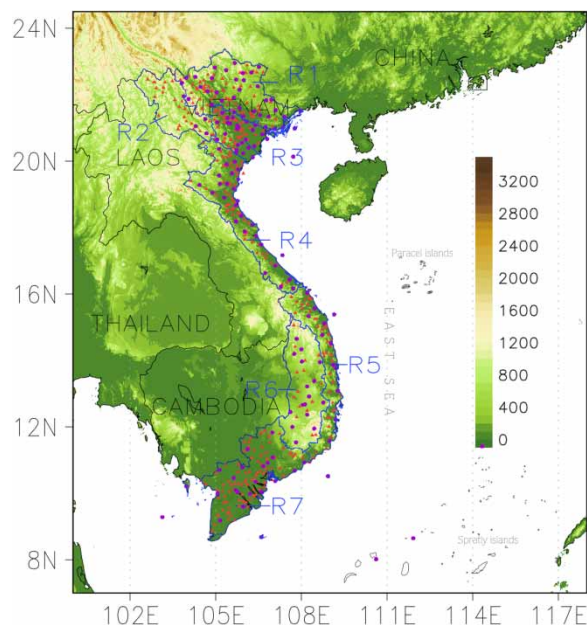


Figure 1 | Seven climatic sub-regions of Vietnam. Data from 157 temperature stations and 481 rainfall stations, indicated by purple and red circles, respectively, were used in this study. Topography over Vietnam (shaded, in m) is obtained from the hydrological data and maps based on Shuttle Elevation Derivatives at multiple Scales (HydroSHEDS) (Lehner *et al.* 2008). Please refer to the online version of this paper to see this figure in color: <http://dx.doi.org/10.2166/wcc.2022.144>.

the sub-regions, which is from April to September for R1, April–October for R2, May–October for R3, R6–R7, and August–December for R4–R5 (Nguyen & Nguyen 2004).

Daily observation data and associated processing method

In this study, near-surface daily average (T_2 m), daily maximum (T_{\max}), and minimum (T_{\min}) temperatures and daily rainfall data from 1980 to 2005 are acquired from the Vietnam Meteorological and Hydrological Administration (VMHA). There are 147 and 481 stations for temperature and rainfall, respectively (Figure 1). The station data are interpolated to a $0.1^\circ \times 0.1^\circ$ gridded dataset by using the Kriging interpolation technique (Switzer 2014) for temperature and the Sphere map interpolation technique (Willmott *et al.* 1985) for rainfall. Nguyen-Xuan *et al.* (2016) showed that the Spheremap interpolation technique has advantages in creating a gridded rainfall dataset over Vietnam in comparison with several other interpolation methods such as Cressman (1959), Inverse Distance Weighted (Shepard 1968), or Kriging (Switzer 2014). Besides, the Kriging technique is an effective interpolation method for continuous spatial variables such as temperature (Wu & Li 2013). The newly-created gridded dataset (hereinafter called OBS) is used in this study to statistically downscale GCM data for Vietnam.

Model data

Daily rainfall (R) and temperatures (T_2 m, T_{\max} , T_{\min}) from 31 CMIP5 GCMs (Table 1) are obtained via the Earth System Grid Federation portal (ESGF, <https://esgf-node.llnl.gov/projects/cmip5/>). The present-day simulations for the period 1980–2005 are used as the basis to construct statistical relationships between the high-resolution OBS dataset and the coarse resolution GCMs. Those relationships are further used to statistically downscale the projected GCM variables for the period 2006–2100 under the RCPs 2.6, 4.5, 6.0, and 8.5.

The BCSD approach

The BCSD approach consists of two stages: BC and SD (Wood 2002; Wood *et al.* 2004) (Figure 2). Firstly, cumulative distribution functions (CDFs) for both observations and historical GCM simulations are separately constructed for each climate variable for each of the 12 months (January–December) within each grid cell. Then, transfer functions that map the

Table 1 | List of 31 CMIP5 GCMs, their resolutions, and RCP availability that are used in this study

No.	Climate Modeling Group	CMIP5 Model ID	Grid resolution (degree)		Availability				
			Lon.	Lat.	RCP 2.6	RCP 4.5	RCP 6.0	RCP 8.5	
1	Commonwealth Scientific and Industrial Research Organization and Bureau of Meteorology, Australia	ACCESS1-0	1.25	1.875	*			*	
2		ACCESS1-3	1.25	1.875		*		*	
3	Beijing Climate Center, China Meteorological Administration	BCC-CSM1-1	2.791	2.813	*	*	*	*	
4		BCC-CSM1-1-M	2.791	2.813	*	*		*	
5	College of Global Change and Earth System Science, Beijing Normal University	BNU-ESM	2.791	2.813	*	*		*	
6	Canadian Centre for Climate Modelling and Analysis	CanESM2	2.791	2.813	*	*		*	
7	National Center for Atmospheric Research	CCSM4	0.942	1.25		*	*	*	
8	Community Earth System Model Contributors	CESM1-BGC	0.942	1.25		*		*	
9		CESM1-CAM5	0.942	1.25	*	*	*	*	
10	Centro Euro-Mediterraneo per I Cambiamenti Climatici	CMCC-CM	0.748	0.75		*		*	
11	Centre National de Recherches Météorologiques/ Centre Européen de Recherche et Formation Avancée en Calcul Scientifique	CNRM-CM5	1.401	1.406	*	*		*	
12	Commonwealth Scientific and Industrial Research Organization, Queensland Climate Change Centre of Excellence	CSIRO-Mk3-6-0	1.865	1.875	*	*	*	*	
13	NOAA Geophysical Fluid Dynamics Laboratory	GFDL-CM3	2	2.5	*	*		*	
14		GFDL-ESM2G	2.023	2	*	*	*	*	
15	NASA Goddard Institute for Space Studies	GISS-E2-H	2	2.5	*	*	*	*	
16		GISS-E2-H-CC	2	2.5		*		*	
17		GISS-E2-R	2	2.5	*	*	*	*	
18		GISS-E2-R-CC	2	2.5		*		*	
19		Met Office Hadley Centre (additional HadGEM2-ES realizations contributed by Instituto Nacional de Pesquisas Espaciais)	HadGEM2-CC	1.25	1.875		*		*
20		HadGEM2-ES	1.25	1.875	*	*		*	
21	Institut Pierre-Simon Laplace	IPSL-CM5A-LR	1.897	3.75	*	*		*	
22		IPSL-CM5A-MR	1.268	2.5	*	*	*	*	
23		IPSL-CM5B-LR	1.895	3.75		*		*	
24	Japan Agency for Marine-Earth Science and Technology, Atmosphere and Ocean Research Institute (The University of Tokyo), and National Institute for Environmental Studies	MIROC-ESM	2.791	2.813	*	*	*	*	
25		MIROC-ESM-CHEM	2.791	2.813		*	*	*	
26	Atmosphere and Ocean Research Institute (The University of Tokyo), National Institute for Environmental Studies, and Japan Agency for Marine-Earth Science and Technology	MIROC5	1.401	1.406	*	*	*	*	
27	Max-Planck-Institut für Meteorologie (Max-Planck Institute for Meteorology)	MPI-ESM-LR	1.865	1.875	*	*		*	
28		MPI-ESM-MR	1.865	1.875	*	*		*	
29	Meteorological Research Institute	MRI-CGCM3	1.121	1.125	*	*		*	
30	Norwegian Climate Centre	NorESM1-M	1.895	2.5	*	*	*	*	
31		NorESM1-ME	1.895	2.5		*		*	
Total number of available models for each RCP						20	31	12	31

* indicates yes.

distribution of simulations onto observations are created (Gudmundsson *et al.* 2012). Next, the biases in the GCM monthly outputs, re-gridded to the intermediate resolution of $1^\circ \times 1^\circ$, are corrected by mapping the quantiles at the same probability between the GCM simulated data and the OBS dataset. Note that previous studies suggested preserving the climatic

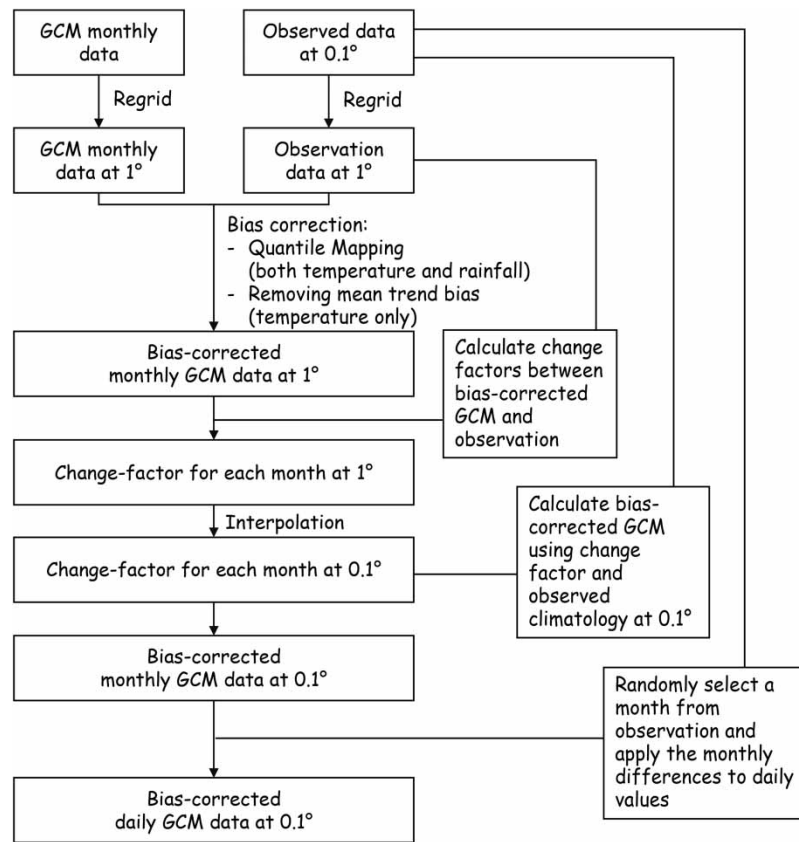


Figure 2 | The schema of the BCSD algorithm applied in this study.

trends in the original GCM (Wood *et al.* 2004; Maurer 2007; Sobie *et al.* 2012); thus, for temperature, the BC is first applied to the detrended data, then the trend at each grid point is added back afterward.

In the second stage, the SD is adopted to spatially translate the BC GCM data from the intermediate resolution of $1^\circ \times 1^\circ$ to the targeted high-resolution of $0.1^\circ \times 0.1^\circ$, by implementing the following steps:

- Change-factors between the GCM BC data and observations are estimated at the intermediate resolution of $1^\circ \times 1^\circ$ for each variable, each model, each month, and each grid cell.

For temperatures, the additive change factor ΔT ($^\circ\text{C}$) is:

$$\Delta T = T_{\text{OBS}} - T_{\text{GCM-BC}} \quad (1)$$

where T represents $T_2 \text{ m}$, T_{max} , or T_{min}

For rainfall, the multiplicative change factor ΔR is:

$$\Delta R = \frac{R_{\text{OBS}}}{R_{\text{GCM-BC}}} \quad (2)$$

Then, the additive and multiplicative change-factors at the intermediate resolution for the reference period are bilinearly interpolated to the targeted high-resolution;

- the high-resolution change-factors are added (for T_{max} , T_{min} , and $T_2 \text{ m}$) or multiplied (for R) to the high-resolution observation climatology to construct the high-resolution downscaled BC monthly climatological fields;

- finally, the BC GCM daily values of a future month are obtained by randomly taking the same month of the observations in the reference period and additively (for temperature) and multiplicatively (for precipitation) adjusting its daily values to reproduce the monthly BC data.

For training and testing the BCSD procedure, we use the split ratio of 60:40 for the reference period 1980–2005, i.e., the first 16 years 1980–1995 (~60% data), called the training period, are used for building the BC transfer functions, and the later 10 years 1996–2005 (~40% data) are used for testing the results. The BCSD-downscaled data obtained for these training and testing periods are called BCSD-CMIP5. Finally, to maximize the construction period of the BCSD approach, following what has been done in previous studies (Reiter *et al.* 2016; Trinh-Tuan *et al.* 2019), the total 26 years period from 1980 to 2005 is used to bias correct and guide the SD for all GCM experiments listed in Table 1 for the future period 2006–2100, to obtain the final downscaled dataset for Vietnam, called CMIP5-VN.

The daily CMIP5-VN dataset, which is about 1.08 Terabytes in size, can be downloaded free of charge at the following address: <http://remosat.usth.edu.vn/~thanhd/Download/CMIP5-VN/>.

The performance of the BCSD-downscaled data for the CMIP5 GCMs, i.e., the BCSD-CMIP5, in representing the observed temporal and spatial distributions is assessed in the next section. We also compare the performance of the BCSD approach with the traditional and effortless bilinear interpolation (BIP) method. Note that the BIP considers the closest 2×2 pixels of each CMIP5 GCM surrounding the unknown pixel's location on the targetted $0.1^\circ \times 0.1^\circ$ grid. Then it computes a weighted average of the values of these four pixels to produce the final interpolated data (hereafter called BIP-CMIP5). The performance comparison between the BCSD and the BIP uses the added value (AV) metric (Di Luca *et al.* 2013):

$$AV = (X_{\text{BIP-CMIP5}} - X_{\text{OBS}})^2 - (X_{\text{BCSD-CMIP5}} - X_{\text{OBS}})^2 \quad (3)$$

where X is one of the four downscaled variables. Accordingly, the higher the AV is, the better the BCSD compares to the BIP.

RESULTS AND DISCUSSION

Performance of the BCSD-CMIP5

We first evaluate the spatial distribution of annual temperature obtained from the simple arithmetic ensemble mean of 31 BCSD-downscaled CMIP5 models (hereafter called BCSD-ENS) over the testing period 1996–2005 (Figure 3(a) and 3(b)). There is a very good agreement between the simulated temperature patterns and observed data. The model ensemble can sensibly resolve the subtle and smooth temperature transition between regions, with a relatively higher temperature in Southern Vietnam and lower temperature in mountainous areas in the North and Central Highlands. The biases, i.e., BCSD-ENS minus OBS, indicated in Figure 3(c)–3(i) and (Figure 3(h)–3(l)) are relatively small, ranging only between -0.36 and 0.56°C (between -0.34 and 0.35°C) throughout the year for the validation (training) period. The average annual bias over Vietnam is 0.05°C for the training period, slightly less than the value of 0.07°C for the testing period. Moreover, the bias patterns seem to appear throughout the regions randomly.

Seasonal temperature biases are generally larger than the annual average bias (Figure 3(c)–(l)). For each season, the temperature bias range is higher in the northern regions (-0.36 to $+0.56^\circ\text{C}$) than in the southern regions (-0.2 to $+0.3^\circ\text{C}$), suggesting that the BC accuracy might be sensitive to the magnitude of annual and seasonal ranges of temperature. As an example, the biases of the BCSD-ENS in June–July–August (JJA, Figure 3(f)) and September–October–November (SON, Figure 3(g)) of the testing period 1996–2005 reached more than 0.2°C in the northern region which is larger than the annual average bias (Figure 3(a)), ranging from -0.1 to 0.1°C . It is worth noting that over the regions with large BCSD-ENS biases, the BC-GCMs generally show a strong agreement in their bias tendency, i.e., at least two-thirds of the model members have the same bias sign as the BCSD-ENS.

The BCSD-ENS biases in maximum and minimum daily temperature (Supplementary material, Figures A1, A2) are relatively higher than those in average daily temperature for both annual and seasonal averages. This can be due to the fact that the input GCM data of the BCSD processes experience larger biases in representing T_{max} and T_{min} compared to $T_2\text{m}$. The average (minimum, maximum) $T_2\text{m}$ bias of the ensemble GCMs over Vietnam is 1.26°C (-3.65°C , 7.61°C) which is smaller than the bias values of 1.56 (-3.95 , 7.64) and 1.99 (-6.50 , 9.32) of T_{max} and T_{min} , respectively (figure not shown). Note that previous studies also indicated large biases of GCMs in addressing daily extreme variables such as T_{max} and T_{min} (Rana *et al.* 2014; Tran Anh & Taniguchi 2018; Panjwani *et al.* 2020). The larger biases in the GCM

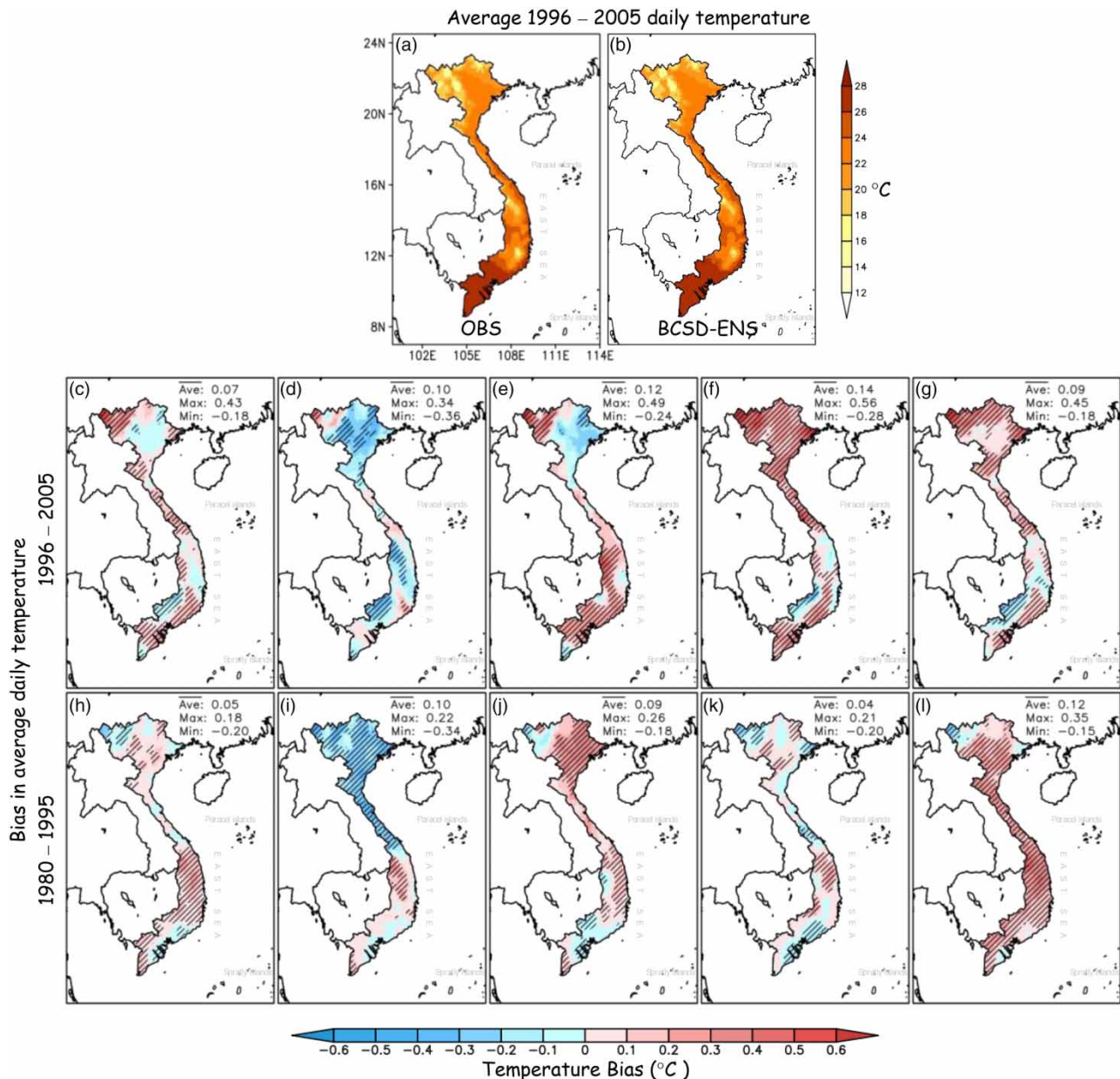


Figure 3 | Spatial distribution of annual average temperature in Vietnam by OBS and BCSD-ENS. (a, b) The average 1996–2005 temperature by OBS and BCSD-ENS; (c–g) and (h–l) indicate the biases of BCSD-ENS compared to OBS for the testing period 1996–2005 and the training period 1980–1995, respectively. The hatching lines show the regions where over two-thirds of CMIP5 models have the same bias sign with BCSD-ENS.

inputs of the BCSD processes potentially exacerbate the output biases, thus inferring the larger BCSD-ENS biases in T_{max} and T_{min} .

The BCSD outputs for precipitation also show a good agreement with OBS, partly illustrated by the average bias of 4.99% for the testing period (Figure 4(a)–4(c)). Locations of the rainfall centers in Vietnam (e.g. in the North, Central, and South of Central Highlands) are well represented by the BCSD-ENS (Figure 4(a) and 4(b)). Although the bias patterns are distributed differently between seasons and regions, the BCSD-ENS in the testing period tends to underestimate precipitation by up to –36% in the South Central, Central Highlands, and South regions and overestimate precipitation by up to 28% in the North, particularly in SON (Figure 4(d)–4(g)). For the training period, the BCSD-ENS results (Figure 4(i)–4(l)), with an annual

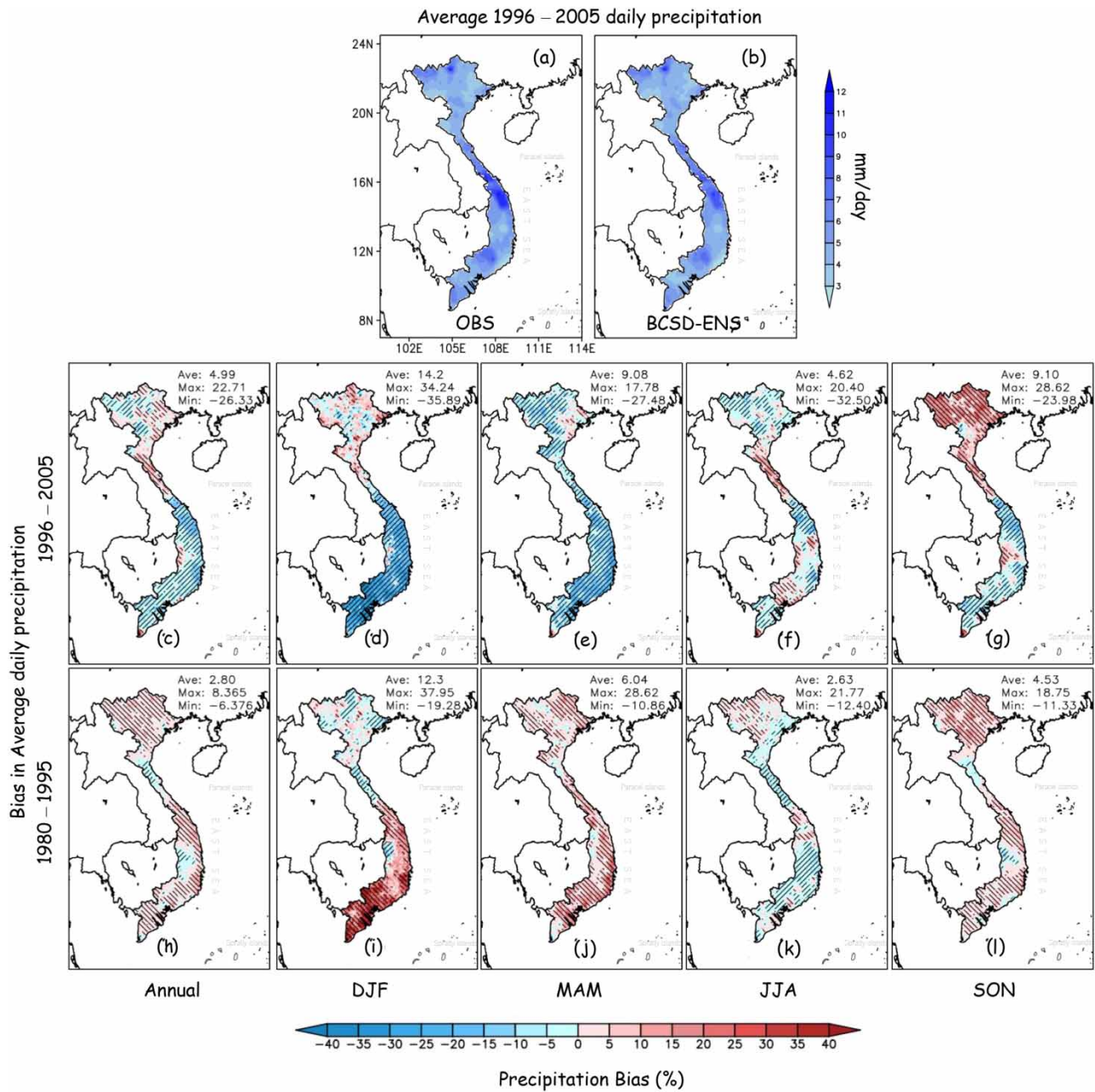


Figure 4 | Spatial distribution of annual average precipitation in Vietnam by OBS and BCSD-ENS. (a, b) The average 1996–2005 precipitation by OBS and BCSD-ENS; (c–g) and (h–l) indicate the biases of BCSD-ENS compared to OBS for the testing period 1996–2005 and the training period 1980–1995, respectively. The hatching lines show the regions where over two-thirds of CMIP5 models have the same bias sign with BCSD-ENS.

average bias of 2.8%, are better than those for the testing period, which is reasonable. Winter season rainfall exhibits the largest bias range among all seasons in the BCSD results for both training (−19.28 to 27.95%) and testing (−35.89 to 34.24%) datasets. Note that the rainfall biases of the BCSD products are still large over some regions. These large values indicate that they are not entirely systematic biases and rainfall highly varies with time and space; therefore, the TFs learned in the training period could hardly be truly applicable in the testing period. From Figure 4, it is worth mentioning that relatively small absolute biases may appear as significant percentage biases in regions and seasons with dry (i.e. little rainfall) conditions, e.g., in December–January–February (DJF).

The ability of the BCSD-ENS in reproducing the seasonal cycle is illustrated in Figure 5, where temporal correlations between the BC outputs and OBS for the testing period are displayed. The average correlation values are very high, i.e., 0.998 and 0.97 for temperature and precipitation, respectively, indicating a good agreement between the BCSD-ENS and OBS (Figure 5(a) and 5(c)). The simple BIP-downscaled CMIP5 GCMs ensemble (BIP-ENS) also shows good seasonal cycles compared to OBS, with average correlations of 0.97 and 0.88 for temperature and precipitation, respectively (Figure 5(c) and 5(d)). It should be noted that the BCSD-ENS exhibits a significantly higher correlation than the BIP-ENS does on all grid points, indicating noticeably better results of the BCSD method in all regions.

The reproducibility of the BCSD outputs for the seasonal cycles of temperature and precipitation are further investigated in Figure 6 by comparing the BCSD-ENS, the BIP-ENS, 31 individual CMIP5 models downscaled by both methods, and OBS

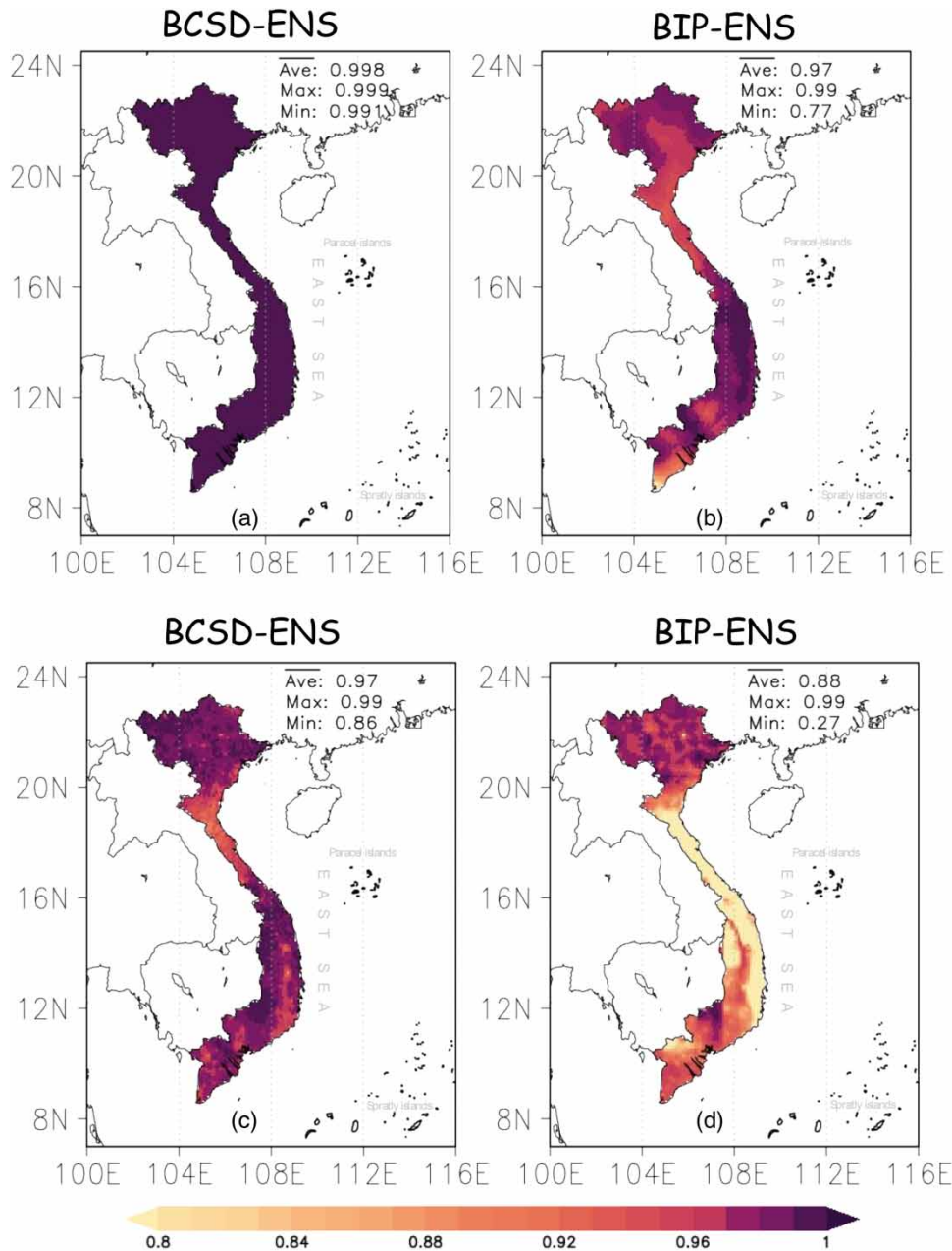


Figure 5 | Temporal correlations of the 1996–2005 seasonal cycles between the BCSD-ENS (left) and BIP-ENS (right) with OBS for (a, b) temperature and (c, d) precipitation.

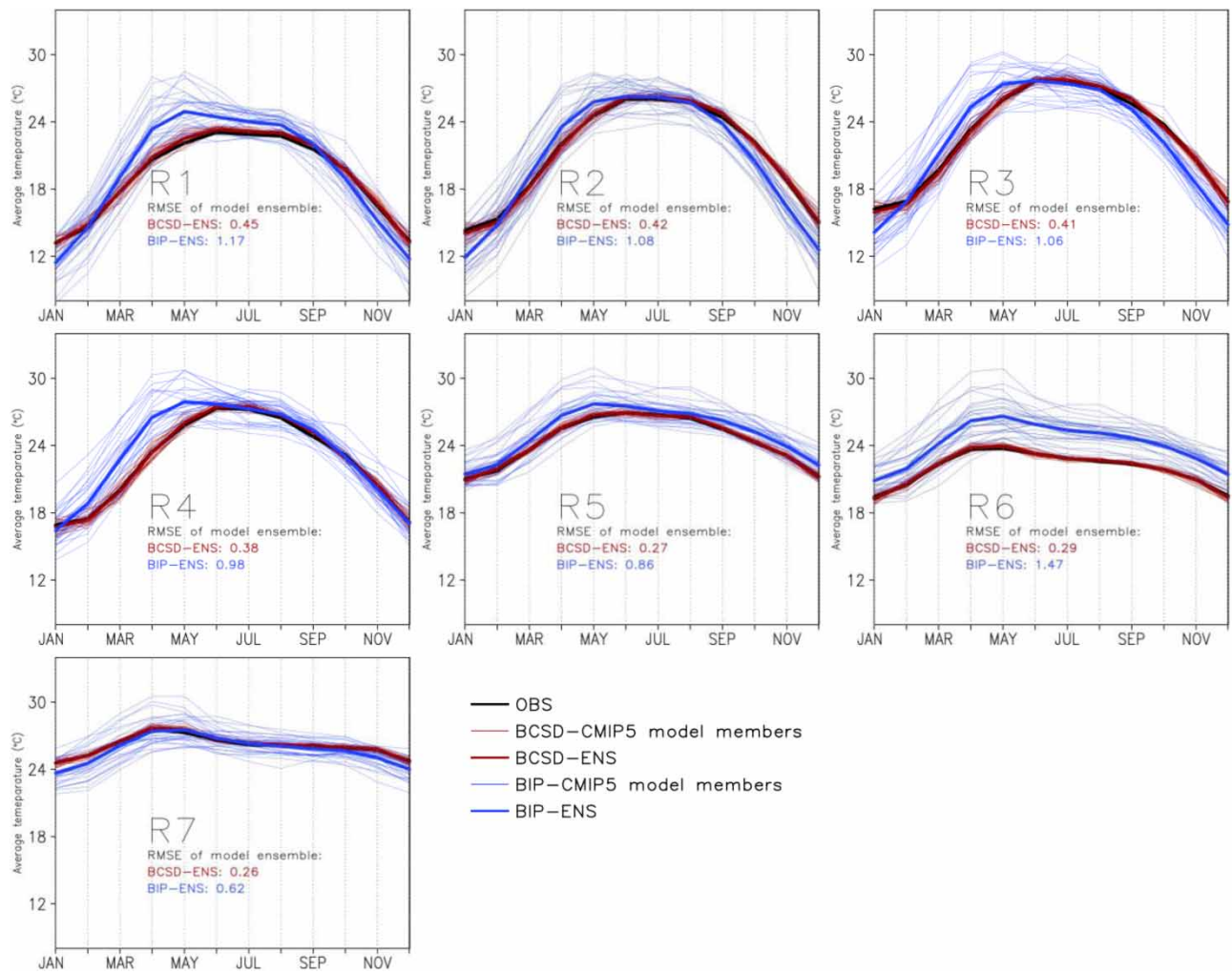


Figure 6 | Comparison of seasonal temperature cycles by OBS, BCSD, and BIP for the seven climatic sub-regions for the period 1996–2005. The seasonal cycle is shown for OBS (black), for 31 downscaled individual CMIP5 model members by BCSD (dim red) and BIP (dim blue), and two models ensemble mean, the BCSD-ENS (dark red) and the BIP-ENS (dark blue). Mean square errors (MSE) of the BCSD-ENS and BIP-ENS are also indicated. Please refer to the online version of this paper to see this figure in color: <http://dx.doi.org/10.2166/wcc.2022.144>.

for all seven climatic sub-regions. Significant agreements in seasonal temperature variation between the BCSD outputs and OBS are clearly illustrated with low root mean square (RMSE) values, ranging from 0.26 °C in the South region to 0.45 °C in the Northwest. While it is difficult to distinguish the seasonal cycles of the BCSD-ENS from OBS, the differences between the BIP-ENS and OBS are clear. The BIP-ENS product generally underestimates autumn-winter rainfall from the Northwest to North Central and consistently overestimates rainfall in the remaining months and regions. Since the variations among the BIP members are much larger than among the BCSD members, the RMSEs of the BIP-ENS results, ranging from 0.62 °C in the South to 1.47 °C in Central Highlands, are much larger than those of the BCSD-ENS.

Figure 7 shows the good performance of the BCSD-downscaled results in reproducing the observed seasonal precipitation cycles. The BCSD outputs can well capture the phase and amplitude of the seasonal cycles over all the climatic sub-regions, including R4 (North Central) and R5 (South Central), where the rainy season comes late in the last months of the year. Both BCSD and BIP downscaling results exhibit higher dispersions in months with higher precipitation amounts. The average RMSEs are relatively small for the BCSD-ENS, ranging from 0.5 mm/day in R1 (Northeast) and R3 (North Delta) to 1.35 mm/day in R5. In all regions, the BCSD RMSEs are significantly lower than BIP (1.0–4.55 mm/day).

Furthermore, the added values of the BCSD downscaling over the simple BIP method are presented by AVs (Equation (3)) shown in Figures 8 and 9 for temperature and precipitation, respectively.

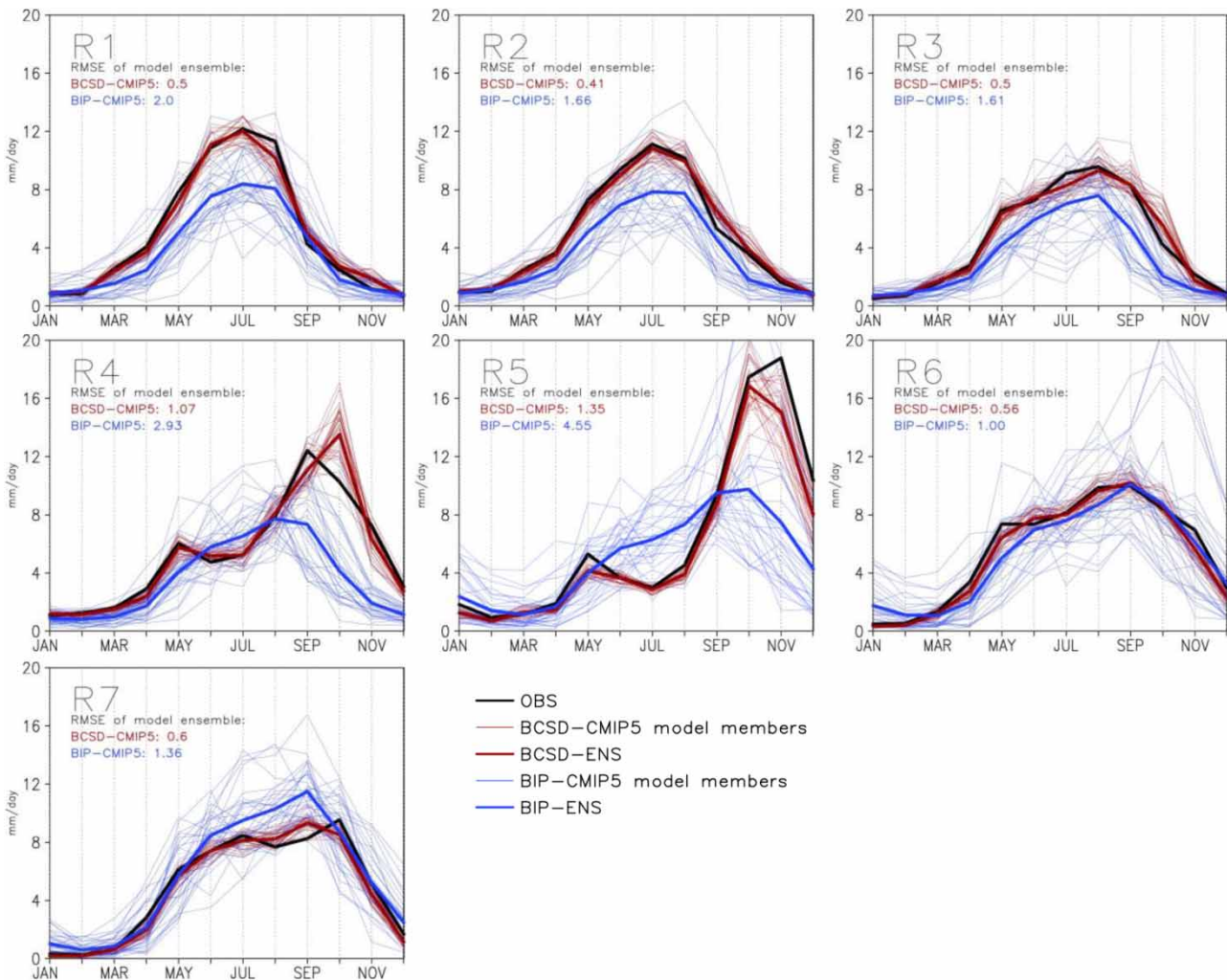


Figure 7 | Comparison of seasonal precipitation cycles by OBS, BCSD, and BIP for the seven climatic sub-regions for the period 1996–2005. The seasonal cycle is shown for OBS (black), for 31 downscaled individual CMIP5 model members by BCSD (dim red) and BIP (dim blue), and two models ensemble mean, the BCSD-ENS (dark red) and the BIP-ENS (dark blue). Mean square errors (MSE) of the BCSD-ENS and BIP-ENS are also indicated. Please refer to the online version of this paper to see this figure in color: <http://dx.doi.org/10.2166/wcc.2022.144>.

The positive AV grids dominate most of the Vietnam territory in all BCSD models' outputs for temperature downscaling, from 94.8% in CSIRO-Mk3-6-0 to 99.3% in NorESM1-M. The BCSD-ENS has 97.3% of grid points with positive AVs. The negative AV range in the models (−1 to 0) is much narrower than the positive range (0–70), suggesting only minor differences between the BCSD and BIP in the locations where the BIP is better than the BCSD (Figure 8).

Over Vietnam, the percentage of positive AV regions for precipitation downscaling in all BCSD-CMIP5 outputs vary from 88.7% in MIROC5 to 97.2% in CMCC-CM (Figure 9). Notably, the BCSD-ENS has 99.9% of grid points with positive AVs. Similar to temperature, the negative AVs vary within the narrow range of (−1 to 0), highlighting minor differences between the BCSD and BIP in those areas (Figure 9).

In summary, this subsection has demonstrated the overwhelming performance of the BCSD downscaling method for temperature and precipitation over Vietnam, even when examining the testing period 1996–2005. For each CMIP5 GCM and the ensemble mean, the BCSD outperforms the simple BIP method over almost all territories of Vietnam.

Future projections

This section presents a preliminary application of the CMIP5-VN in assessing future climate changes over Vietnam and its seven climate sub-regions.

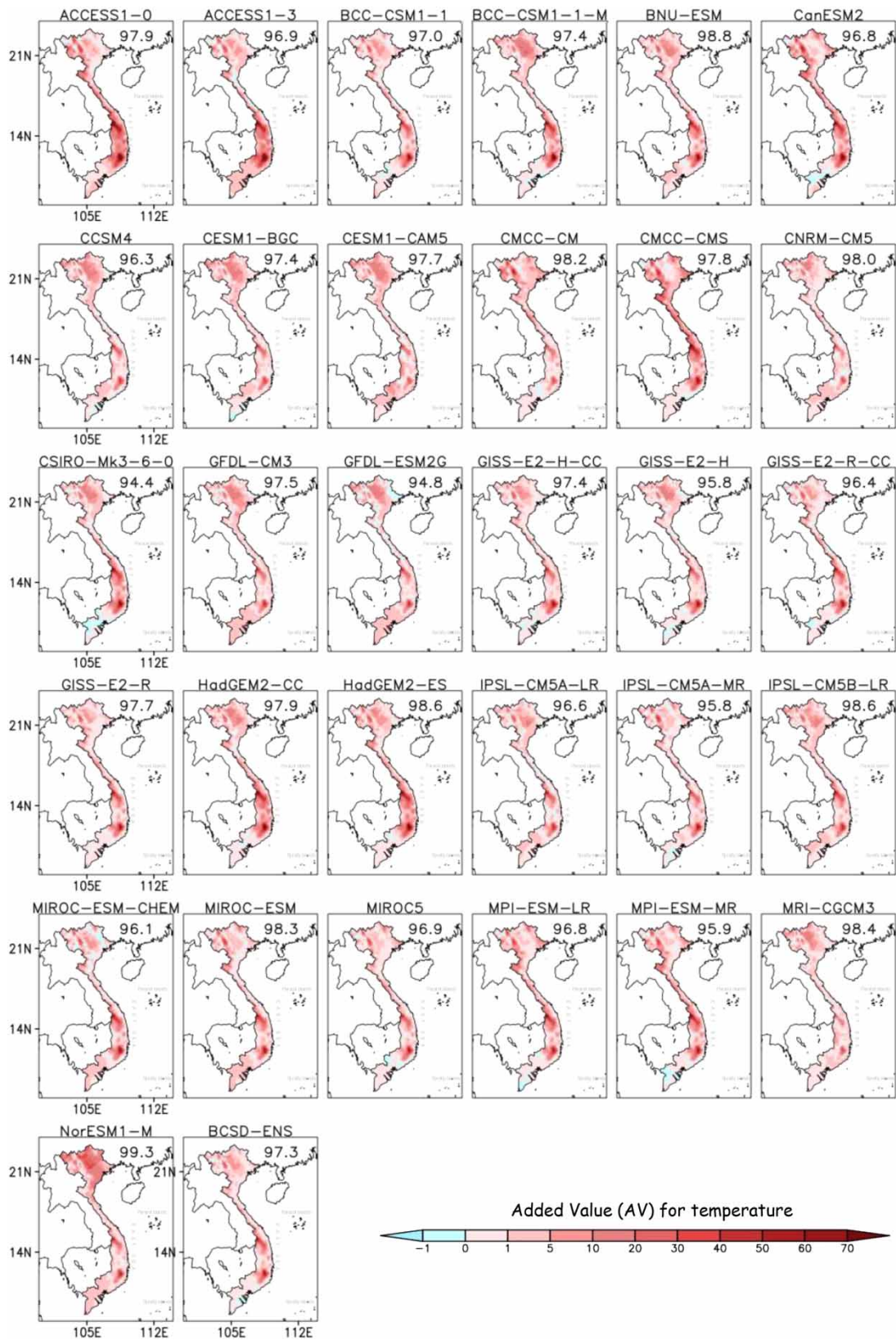


Figure 8 | AVs of individual BCSD-CMIP5 and BCSD-ENS for temperature over the BIP-CMIP5 for the 1996-2005 period. The darker saturation of warm/cold color denotes the more skillful/unskillful of the BCSD. The number in the top right corner indicates the percentage of the grids having positive AVs.

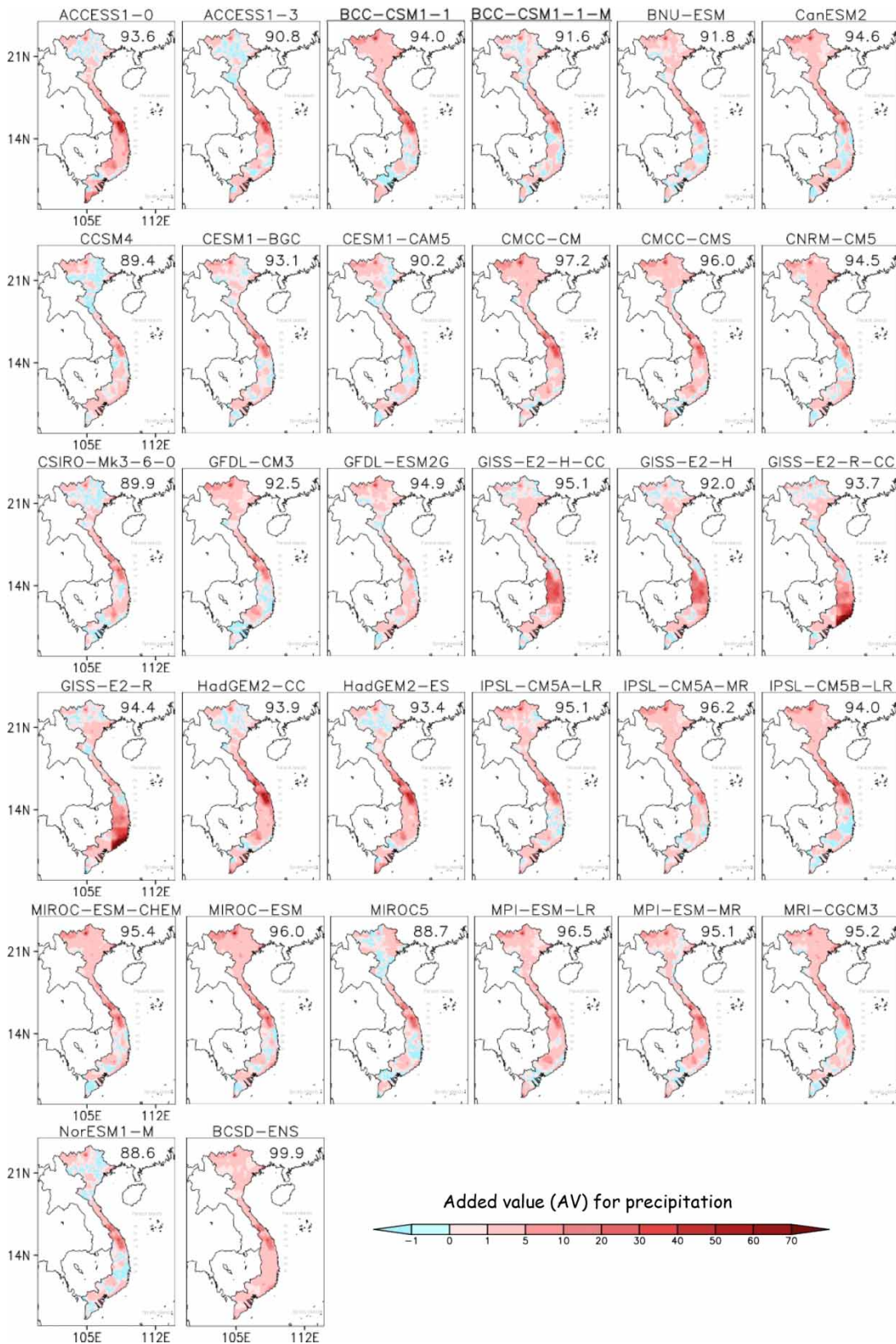


Figure 9 | AVs of individual BCSD-CMIP5 and BCSD-ENS for precipitation over the BIP-CMIP5 for the 1996–2005 period. The darker saturation of warm/cold color denotes the more skillful/unskillful of the BCSD. The number in the top right corner indicates the percentage of the grids having positive AVs.

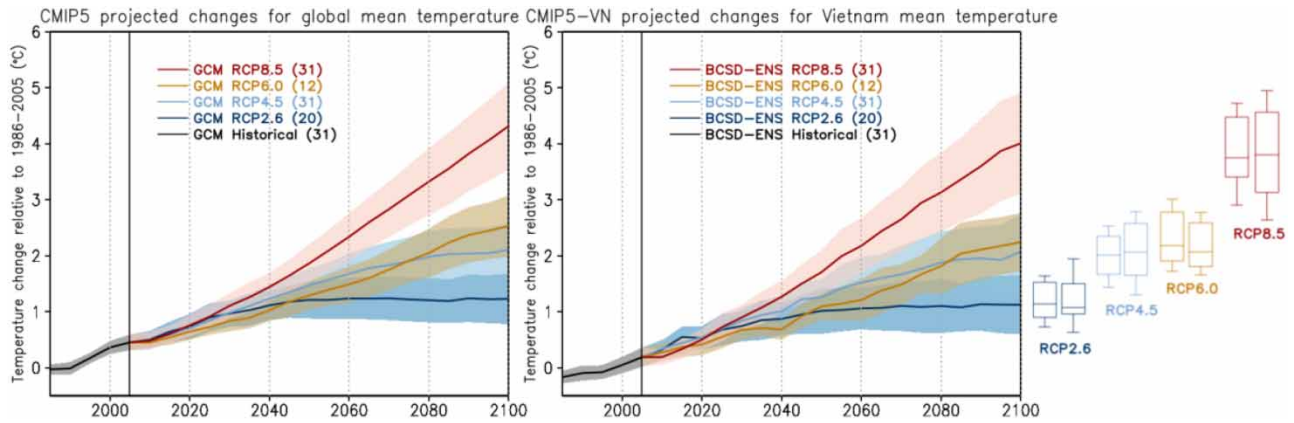


Figure 10 | Projected temperature changes relative to the baseline period 1986–2005 based on the CMIP5 GCMs and BCSD-CMIP5 data for global average (left) and Vietnam (right), respectively. Five-year moving averages are applied. Colored lines show the ensemble means of the models and colored shaded areas present the uncertainty ranges (± 1 standard deviation) for each RCP. The number of models used for each RCP is shown in brackets. Box plots on the right display the occurrence statistics (quartile, median, 10th, and 90th percentile) for warming levels on the global scale (left boxes) and in Vietnam (right boxes) at the end of the 21st century 2080–2099.

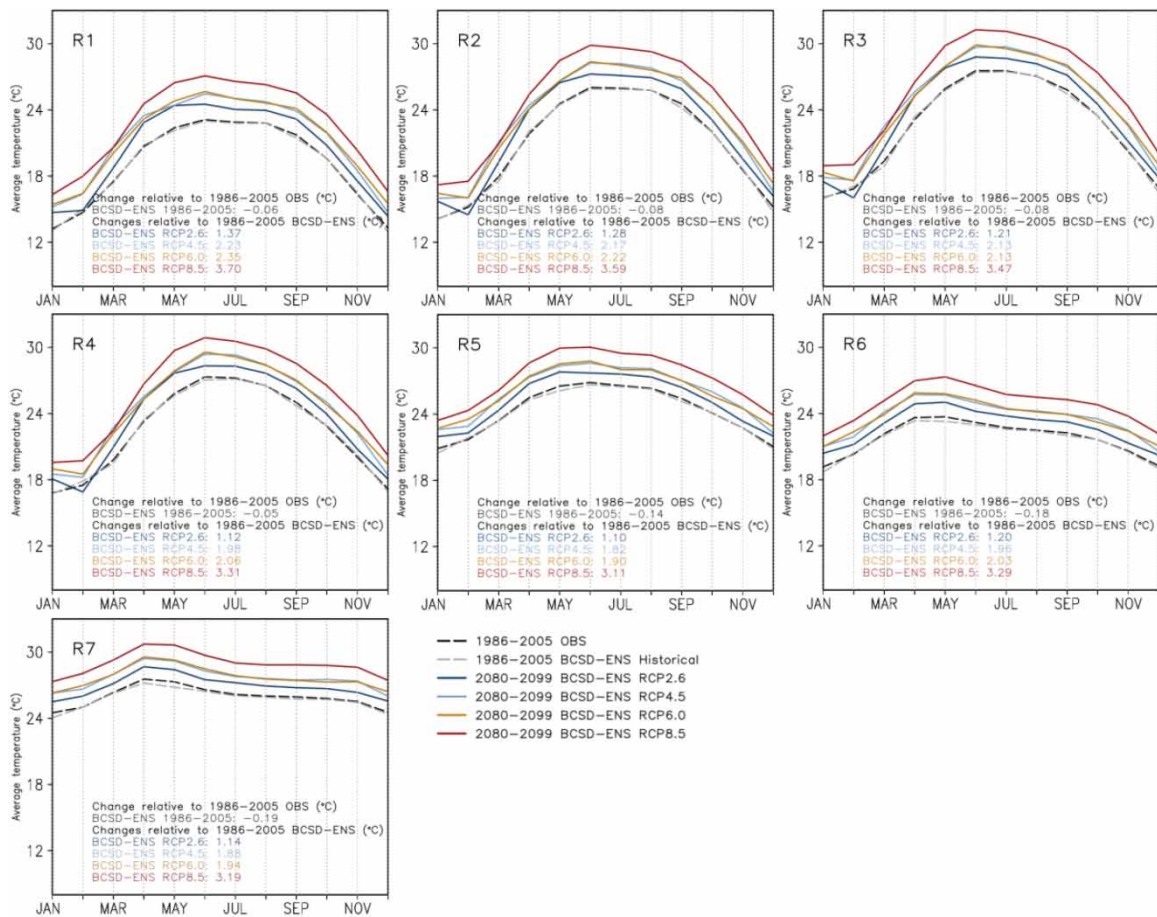


Figure 11 | Comparison between the seasonal temperature cycles of the BCSD-ENS and OBS over the seven climatic sub-regions of Vietnam. Black and grey dashed lines, respectively, represent the OBS and BCSD-ENS cycles for 1986–2005, while color lines represent the future 2080–2099 seasonal cycles for each RCP. Average changes between the future 2080–2099 BCSD-ENS and the 1986–2005 OBS with the historical 1986–2005 BCSD-ENS are also displayed. Please refer to the online version of this paper to see this figure in color: <http://dx.doi.org/10.2166/wcc.2022.144>.

Future global (obtained from the CMIP5 GCMs) and Vietnam (obtained from the CMIP5-VN) warming levels over the 21st century compared to the baseline period 1986–2005 are displayed in Figure 10. While the average warming trends in Vietnam are slightly smaller, the warming variability in Vietnam is larger than the global average for all RCPs at the end of the century. The average temperature in Vietnam increases by 1.3 ± 0.52 °C under RCP2.6 and by 3.85 ± 0.85 °C under RCP8.5. The model variability for each RCP is generally larger in Vietnam than that of the global scale except for the RCP6.0 scenario, which has a limited number of models. It is worth mentioning that our results for Vietnam are aligned with the latest IPCC AR6, which concluded with high confidence that future warming in Southeast Asia (including Vietnam) will be slightly less than the global average (Gutiérrez *et al.* 2021).

The progress of global warming in the seven climatic sub-regions of Vietnam at the end of the 21st century is illustrated in Figure 11, where the BCSD-ENS temperature seasonal cycles of the future 2080–2099 and baseline 1986–2005 periods are compared. Results indicate that regional mean temperatures, which vary between regions, are projected to increase by 1.10–1.37 °C under RCP2.6 and by 3.11–3.70 °C under RCP8.5. The warming in the northern regions (R1–R4) is more intense than in the south (R5–R7), by 0.10 and 0.31 °C warmer on average under RCP2.6 and RCP8.5, respectively. In the northern

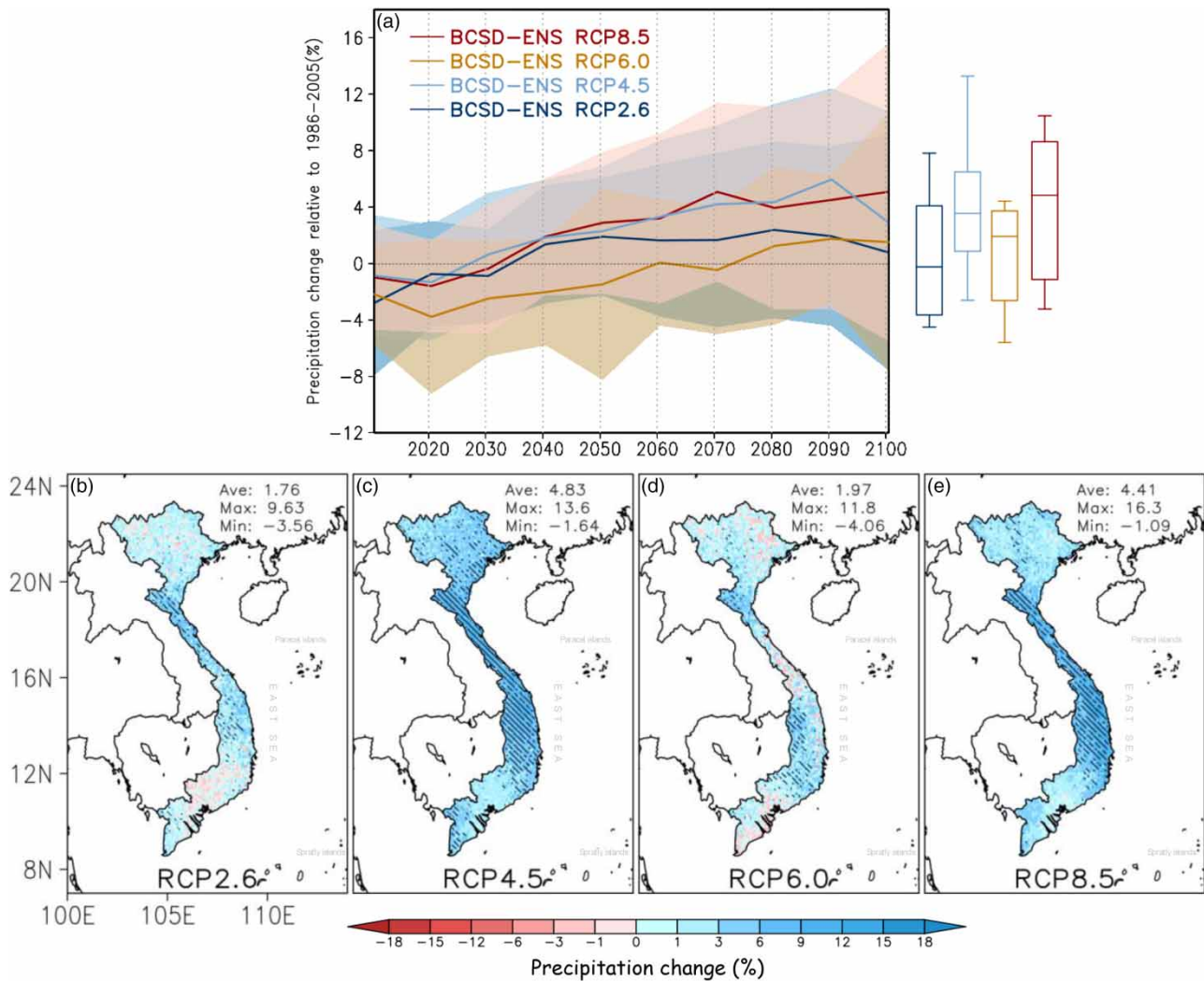


Figure 12 | Projected precipitation changes in Vietnam under different RCPs. (a) Colored lines present the 10-year moving average of the BCSD-ENS and colored shaded areas show the uncertainty ranges (± 1 standard deviation). Box plots on the right display the occurrence statistics (quartile, median, 10th, and 90th percentile) for precipitation changes at the end of the 21st century 2080–2099. (b–e) Distribution of change patterns between the 2080–2099 and 1986–2005 periods derived by the BCSD-ENS. The hatching lines show the regions where over two-thirds of BCSD-CMIP5 models have the same bias sign as the BCSD-ENS.

regions, projected temperature increases are about 0.44–0.76 °C higher in summer than in winter for all RCPs. Our findings here correlate well with MONRE (2016)'s results, which were based on a limited number of dynamical downscaling experiments.

Projection of CMIP5-VN precipitation change in Vietnam related to the 1986–2005 period is illustrated in Figure 12. Contrary to the clear increasing temperature trends across all models, the trends of precipitation contain more uncertainties (Figure 12(a)). The average precipitation in the far future 2080–2099 is projected to generally increase by $1.16 \pm 7.1\%$ under RCP2.6 and by $4.41 \pm 9.2\%$ under RCP8.5. The uncertainties increase with time and are highest under the high GHG concentration scenario RCP8.5. Over the whole of Vietnam, the BCSD-ENS shows a slight increasing precipitation trend, except for some small areas in the North and South (Central Vietnam) under RCP2.6 (RCP6.0) (Figure 12(b)–12(e)). There is a more robust agreement of the CMIP5-VN products on the increasing precipitation trend in Central Vietnam (including R4 and the northern parts of R5 and R6) under RCP4.5 and RCP8.5 than in the remaining regions and scenarios.

The slight changes in the projected mean precipitation at the end of the 21st century are also demonstrated by the slight increases in the average seasonal precipitation over the seven climatic sub-regions (Figure 13). The average changes of the BCSD-ENS vary from 0.31 to 3.54% under RCP2.6 and from 2.10 to 9.50% under RCP8.5. In the dry months, only a small increase or decrease in future rainfall can cause a large percentage change. For example, the BCSD-ENS rainfall is projected to increase by 35% in February under RCP6.0 and to decrease by –25% in March under RCP8.5 in the South region (R7); however, the average monthly rainfall values of R7 in these months are less than 0.5 mm/day, which are very small.

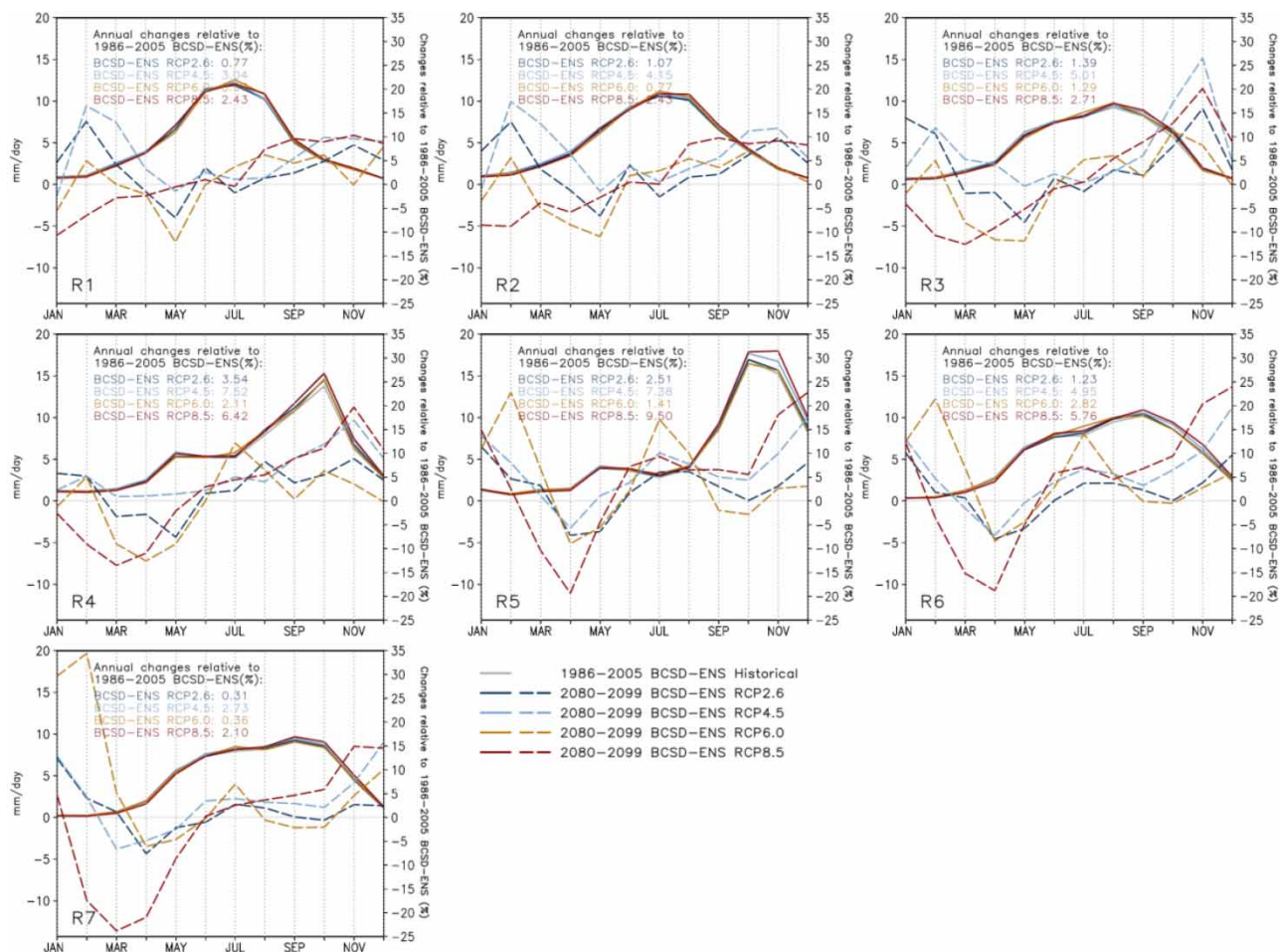


Figure 13 | Precipitation seasonal cycles (left axis, solid lines) under different RCPs and their percentage changes (right axis, dash lines) relative to the 1986–2005 BCSD-ENS over the seven climatic sub-regions of Vietnam. Average changes (%) of the BCSD-ENS between the future 2080–2099 and the baseline 1986–2005 period are also displayed.

There is a tendency of rainfall reduction in the dry months, particularly during March–April–May, suggesting that dry conditions are exacerbated in the future, especially under RCP8.5. On the other hand, more rainfall is projected from June to the end of the year in most climatic sub-regions under all RCPs. In particular, rainfall is projected to increase under RCP4.5 and RCP8.5 by more than 10% in North Central (R4), and by 5–20% in South Central (R5) from September to November, which are the months with the highest rainfall of the year, suggesting more extreme rainfall events in the future in these regions.

CONCLUSIONS

In this study, the high-resolution (10 km) daily temperature (including near-surface daily average, daily maximum, and minimum temperatures) and precipitation dataset for Vietnam, called CMIP5-VN, has been successfully developed by applying the BCSO method for 31 CMIP5 GCMs for the baseline period 1980–2005 and the future period 2006–2100 under four GHG concentration scenarios RCP2.6, RCP4.5, RCP6.0, and RCP8.5.

With the newly-built CMIP5-VN dataset, future scenarios for Vietnam are not only limited to RCP4.5 and RCP8.5 as shown in previous studies (e.g. MONRE 2016, 2021; Trinh-Tuan *et al.* 2019) but also available for RCP2.6 and RCP6.0. The CMIP5-VN is recommended for studies on climate change assessment and climate change impacts in Vietnam.

As outputs of CMIP6 GCMs have recently become available on the ESGF, future studies will therefore need to downscale, both statistically and dynamically, the CMIP6 outputs for the region. Furthermore, it should also be noted that the CMIP5 and CMIP6 results may not cover all probabilities that could occur in the future. Thus, a study that applies the probabilistic method suggested by Rasmussen *et al.* (2016) and Hsiang *et al.* (2017) could be considered to build a next climate change dataset for Vietnam. This new approach is expected to better depict the tails of the probability distribution and, therefore, could better project the extreme risks that may occur in the future.

AUTHORS' CONTRIBUTIONS

Q.T.-A., T.N.-D., and E.E. conceptualized the research. Q.T.-A. carried out the downscaling experiments and performed the analysis. L.T.-T. processed and prepared the observation data. Q.T.A. and T.N.-D. drafted the manuscript. All authors discussed the results and commented on the manuscript.

FUNDING

This work belongs to the CLIMATO package of the GEMMES Vietnam project, launched by the French Development Agency (AFD).

DATA AVAILABILITY STATEMENT

All relevant data are included in the paper or its Supplementary Information.

CONFLICT OF INTEREST

The authors declare there is no conflict.

REFERENCES

- Arias, P. A., Bellouin, N., Coppola, E., Jones, R. G., Krinner, G., Marotzke, J., Naik, V., Palmer, M. D., Plattner, G.-K., Rogelj, J., Rojas, M., Sillmann, J., Storelmo, T., Thorne, P. W., Trewin, B., Achuta Rao, K., Adhikary, B., Allan, R. P., Armour, K., Bala, G., Barimalala, R., Berger, S., Canadell, J. G., Cassou, C., Cherchi, A., Collins, W., Collins, W. D., Connors, S. L., Corti, S., Cruz, F., Dentener, F. J., Dereczynski, C., Di Luca, A., Diongue Niang, A., Doblak-Reyes, F. J., Dosio, A., Douville, H., Engelbrecht, F., Eyring, V., Fischer, E., Forster, P., Fox-Kemper, B., Fuglestedt, J. S., Fyfe, J. C., Gillett, N. P., Goldfarb, L., Gorodetskaya, I., Gutierrez, J. M., Hamdi, R., Hawkins, E., Hewitt, H. T., Hope, P., Islam, A. S., Jones, C., Kaufman, D. S., Kopp, R. E., Kosaka, Y., Kossin, J., Krakovska, S., Lee, J.-Y., Li, J., Mauritsen, T., Maycock, T. K., Meinshausen, M., Min, S.-K., Monteiro, P. M. S., Ngo-Duc, T., Otto, F., Pinto, I., Pirani, A., Raghavan, K., Ranasinghe, R., Ruane, A. C., Ruiz, L., Sallée, J.-B., Samset, B. H., Sathyendranath, S., Seneviratne, S. I., Sörensson, A. A., Szopa, S., Takayabu, I., Tréguier, A.-M., van den Hurk, B., Vautard, R., von Schuckmann, K., Zaehle, S., Zhang, X. & Zickfeld, K. 2021 Technical summary. In: *Climate Change 2021: The Physical Science Basis. Contribution of Working Group I to the Sixth Assessment Report of the Intergovernmental Panel on Climate Change* (Masson-Delmotte, V., Zhai, P., Pirani, A., Connors, S. L., Péan, C., Berger, S., Caud, N., Chen, Y., Goldfarb, L., Gomis, M. I., Huang, M., Leitzell, K., Lonnoy, E., Matthews, J. B. R., Maycock, T. K., Waterfield, T.,

- Yelekçi, O., Yu, R. & Zhou, B., eds). Cambridge University Press, Cambridge, United Kingdom; New York, NY, USA, pp. 33–144, <https://doi.org/10.1017/9781009157896.002>.
- Cressman, G. P. 1959 *An operational objective analysis system*. *Mon. Weather Rev.* **87**, 367–374. [http://dx.doi.org/10.1175/1520-0493\(1959\)087<0367:AOOAS>2.0.CO;2](http://dx.doi.org/10.1175/1520-0493(1959)087<0367:AOOAS>2.0.CO;2)
- Déqué, M., Somot, S., Sanchez-Gomez, E., Goodess, C. M., Jacob, D., Lenderink, G. & Christensen, O. B. 2012 *The spread amongst ENSEMBLES regional scenarios: regional climate models, driving general circulation models and interannual variability*. *Clim. Dyn.* **38** (5–6), 951–964. <https://doi.org/10.1007/s00382-011-1053-x>.
- Diaconescu, E. P. & Laprise, R. 2013 *Can added value be expected in RCM simulated large scales?* *Clim. Dyn.* **41**, 1769–1800. <https://doi.org/10.1007/s00382-012-1649-9>.
- Di Luca, A., de Elfa, R. & Laprise, R. 2013 *Potential for small scale added value of RCM's downscaled climate change signal*. *Clim. Dyn.* **40**, 601–618. <https://doi.org/10.1007/s00382-012-1415-z>.
- Eum, H. I., Cannon, A. J. & Murock, T. Q. 2017 *Intercomparison of multiple statistical downscaling methods: multi-criteria model selection for South Korea*. *Stochastic Environ. Res. Risk Assess.* **31**, 683–703. <https://doi.org/10.1007/s00477-016-1312-9>.
- Eyring, V., Bony, S., Meehl, G. A., Senior, C. A., Stevens, B., Stouffer, R. J. & Taylor, K. E. 2016 *Overview of the Coupled Model Intercomparison Project Phase 6 (CMIP6) experimental design and organization*. *Geosci. Model Dev.* **9**, 1937–1958. <https://doi.org/10.5194/gmd-9-1937-2016>.
- Fowler, H. J., Blenkinsop, S. & Tebaldi, C. 2007 *Linking climate change modelling to impacts studies: recent advances in downscaling techniques for hydrological modelling*. *Int. J. Climatol.* **27**, 1547–1578. <https://doi.org/10.1002/joc.1556>.
- Giorgi, F. & Bi, X. Q. 2009 *Time of emergence (TOE) of GHG-forced precipitation change hot-spots*. *Geophys. Res. Lett.* **36**(6), L06709. doi: <https://doi.org/10.1029/2009GL037593>.
- Giorgi, F. & Gutowski Jr, W. J. 2015 *Regional dynamical downscaling and the CORDEX initiative*. *Annu. Rev. Environ. Resour.* **40** (1), 467–490. <https://doi.org/10.1146/annurev-environ-102014-021217>.
- Gudmundsson, L., Bremnes, J. B., Haugen, J. E. & Engen-Skaugen, T. 2012 *Technical note: downscaling RCM precipitation to the station scale using statistical transformations – a comparison of methods*. *Hydrol. Earth Syst. Sci.* **16**, 3383–3390. <https://doi.org/10.5194/hess-16-3383-2012>.
- Gutiérrez, J. M., Jones, R. G., Narisma, G. T., Alves, L. M., Amjad, M., Gorodetskaya, I. V., Grose, M., Klutse, N. A. B., Krakovska, S., Li, J., Martínez-Castro, D., Mearns, L. O., Mernild, S. H., Ngo-Duc, T., van den Hurk, B., Yoon, J. H., 2021 Atlas. In: *Climate Change 2021: The Physical Science Basis. Contribution of Working Group I to the Sixth Assessment Report of the Intergovernmental Panel on Climate Change* (Masson-Delmotte, V., Zhai, P., Pirani, A., Connors, S. L., Péan, C., Berger, S., Caud, N., Chen, Y., Goldfarb, L., Gomis, M. I., Huang, M., Leitzell, K., Lonnoy, E., Matthews, J. B. R., Maycock, T. K., Waterfield, T., Yelekçi, O., Yu, R. & Zhou, B., eds). Cambridge University Press, Cambridge, United Kingdom; New York, NY, USA, pp. 1927–2058, <https://doi.org/10.1017/9781009157896.021>.
- Hsiang, S., Kopp, R., Jina, A., Rising, J., Masson-Delmotte, V., Zhai, P., Pirani, A., Connors, S. L., Péan, C., Berger, S., Caud, N., Chen, Y., Goldfarb, L., Gomis, M. I., Huang, M., Leitzell, K., Lonnoy, E., Matthews, J. B. R., Maycock, T. K., Waterfield, T., Yelekçi, O., Yu, R. & Zhou, B. (eds). 2017 *Estimating economic damage from climate change in the United States*. *Science* **356** (6345), 1362–1369. <https://doi.org/10.1126/science.aal4369>.
- IPCC 2013 *Climate change 2013: the physical science basis*. In: *Contribution of Working Group I to the Fifth Assessment Report of the Intergovernmental Panel on Climate Change* (Stocker, T. F., Qin, D., Plattner, G.-K., Tignor, M., Allen, S. K., Boschung, J., Nauels, A., Xia, Y., Bex, V. & Midgley, P. M., eds). Cambridge University Press, Cambridge, United Kingdom; New York, NY, USA, p. 1535.
- Lehner, B., Verdin, K. & Jarvis, A. 2008 *New global hydrography derived from spaceborne elevation data*. *Eos, Trans.* **89** (10), 93–94. Available from: <https://www.hydrosheds.org>.
- Maurer, E. P. 2007 *Uncertainty in hydrologic impacts of climate change in the Sierra Nevada, California under two emissions scenarios*. *Clim. Change* **82** (3–4), 309–325. <https://doi.org/10.1007/s10584-006-9180-9>.
- Maurer, E. P. & Hidalgo, H. G. 2008 *Utility of daily vs. monthly large-scale climate data: an intercomparison of two statistical downscaling methods*. *Hydrol. Earth Syst. Sci.* **12**, 551–563. <https://doi.org/10.5194/hess-12-551-2008>.
- Milly, P. C. D., Julio, B., Malin, F., Robert, M. H., Zbigniew, W. Z., Dennis, P.L. & Ronald, J. S. 2008 *Climate change - stationarity is dead: whither water management?* *Science* **319**(5863), 573–574. <https://doi.org/10.1126/science.1151915>.
- MONRE 2009 *Climate Change, Sea Level Rise Scenarios for Vietnam*. Vietnam Natural Resources, Environment and Mapping Publishing House, Hanoi, Vietnam, p. 34.
- MONRE 2012 *Climate Change, Sea Level Rise Scenarios for Vietnam*. Vietnam Natural Resources, Environment and Mapping Publishing House, Hanoi, Vietnam, p. 98.
- MONRE 2016 *Climate Change, Sea Level Rise Scenarios for Viet Nam, Summary for Policy Makers*. Vietnam Natural Resources, Environment and Mapping Publishing House, Hanoi, Vietnam, p. 39.
- MONRE 2021 *Climate Change, Sea Level Rise Scenarios for Viet Nam*. Vietnam Natural Resources, Environment and Mapping Publishing House, Hanoi, Vietnam, p. 144.
- Moss, R., Edmonds, J., Hibbard, K., Manning, M., Rose, K., van Vuuren, D., Carter, T., Emori, S., Kainuma, M., Kram, T., Meehl, G., Mitchell, F. B., Nakicenovic, N., Riahi, K., Smith, S., Stouffer, R., Thomson, A., Weyant, P. & Wilbanks, T. 2010 *The next generation of scenarios for climate change research and assessment*. *Nature* **463**, 747–756. <https://doi.org/10.1038/nature08823>.

- Murphy, J. 1999 An evaluation of statistical and dynamical techniques for downscaling local climate. *J. Clim.* **12** (8), 2256–2284. [https://doi.org/10.1175/1520-0442\(1999\)012<2256:AEOSAD>2.0.CO;2](https://doi.org/10.1175/1520-0442(1999)012<2256:AEOSAD>2.0.CO;2).
- Nguyen, D. N. & Nguyen, T. H. 2004 *Vietnamese Climate and Climatic Resources*. Science and Technology Publishing House, Vietnam, p. 230, (in Vietnamese).
- Nguyen-Thuy, H., Ngo-Duc, T., Trinh-Tuan, L., Tangang, F., Cruz, F., Phan-Van, T., Juneng, L., Narisma, G. & Santisirisomboon, J. 2021 Time of emergence of climate signals over Vietnam detected from the CORDEX-SEA experiments. *Int. J. Climatol.* **41**, 1599–1618. <https://doi.org/10.1002/joc.6897>.
- Nguyen-Xuan, T., Ngo-Duc, T., Kamimera, H., Trinh-Tuan, L., Matsumoto, J., Inoue, T. & Phan-Van, T. 2016 The Vietnam Gridded Precipitation (VnGP) dataset: construction and validation. *SOLA* **12**, 291–296. <https://doi.org/10.2151/sola.2016-057>.
- Noël, T., Harilaos, L., Dimitri, D., Mathieu, V. & Guillaume, L. 2021 A high-resolution downscaled CMIP5 projections dataset of essential surface climate variables over the globe coherent with the ERA5 reanalysis for climate change impact assessments. *Data in Brief* **35**, 106900. <https://doi.org/10.1016/j.dib.2021.106900>.
- Panjwani, S., Naresh Kumar, S., Ahuja, L. & Islam, A. 2020 Evaluation of selected global climate models for extreme temperature events over India. *Theor. Appl. Climatol.* **140**, 731–738. <https://doi.org/10.1007/s00704-020-03108-4>.
- Phan, V. T., Ngo-Duc, T. & Ho, T. M. H. 2009 Seasonal and interannual variations of surface climate elements over Vietnam. *Clim. Res.* **40**, 49–60. <https://doi.org/10.3354/cr00824>.
- Rana, A., Foster, K., Thomas, B., Jonas, O. & Lars, B. 2014 Impact of climate change on rainfall over Mumbai using distribution-based scaling of global climate model projections. *J. Hydrol. Reg. Stud.* **1**, 107–128. <https://doi.org/10.1016/j.ejrh.2014.06.005>.
- Rasmussen, D., Meinshausen, M. & Kopp, R. E. 2016 Probability-weighted ensembles of U.S. county-level climate projections for climate risk analysis. *J. Appl. Meteorol. Climatol.* **55**, 2301–2322. <https://doi.org/10.1175/JAMC-D-15-0302.1>.
- Reiter, P., Gutjahr, O., Schefczyk, L., Heinemann, G. & Casper, M. 2016 Bias correction of ENSEMBLES precipitation data with focus on the effect of the length of the calibration period. *Meteorol. Z.* **25** (1), 85–96. <https://doi.org/10.1127/metz/2015/0714>.
- Salathé Jr, E. P. 2003 Comparison of various precipitation downscaling methods for the simulation of streamflow in a rainshadow river basin. *Int. J. Climatol.* **23**, 887–901. <https://doi.org/10.1002/joc.922>.
- Seaby, L. P., Refsgaard, J. C., Sonnenborg, T. O., Stisen, S., Christensen, J. H. & Jensen, K. H. 2013 Assessment of robustness and significance of climate change signals for an ensemble of distribution-based scaled climate projections. *J. Hydrol.* **486**, 479–493. <https://doi.org/10.1016/j.jhydrol.2013.02.015>.
- Shepard, D. 1968 A two-dimensional interpolation function for irregularly-spaced data. In *Proc. 1968 ACM Nat'l. Conf.* pp. 517 – 524. <https://doi.org/10.1145/800186.810616>.
- Sobie, S. R., Werner, A. T., Murdock, T. Q., Bürger, G. & Cannon, A. J. 2012 Downscaling extremes – an intercomparison of multiple statistical methods for present climate. *J. Clim.* **25**, 4366. – 4388. <https://doi.org/10.1175/JCLI-D-11-00408.1>.
- Switzer, P., 2014 Kriging. In: *Wiley StatsRef: Statistics Reference Online* (Balakrishnan, N., Colton, T., Everitt, B., Piegorsch, W., Ruggeri, F. & Teugels, J. L., eds). <https://doi.org/10.1002/9781118445112.stat03708>.
- Tamara, J., McGrath, F., Macadam, I. & Jones, R. 2019 High-resolution climate projections for South Asia to inform climate impacts and adaptation studies in the Ganges–Brahmaputra–Meghna and Mahanadi deltas. *Sci. Total Environ.* **650**, 1499–1520. <https://doi.org/10.1016/j.scitotenv.2018.08.376>.
- Tangang, F., Chung, J. X., Juneng, L., Supari, S., Ngai, E., Jamaluddin, S. T., Mohd, A. F., Cruz, M. S. F., Narisma, F., Santisirisomboon, G., Ngo-Duc, J., Tan, T., Singhruck, P. V., Gunawan, P., Aldrian, D., Sopaheluwakan, E., Grigory, A., Remedio, N., Sein, A. R. C., Hein-Griggs, D. V., McGregor, D., Yang, J. L., Sasaki, H. & Kumar, H. 2020 Projected future changes in rainfall in Southeast Asia based on CORDEX-SEA multi-model simulations. *Clim. Dyn.* **55** (5), 1247–1267. <https://doi.org/10.1007/s00382-020-05322-2>.
- Taylor, K. E., Stouffer, R. J. & Meehl, G. A. 2012 An overview of CMIP5 and the experiment design. *Bull. Am. Meteorol. Soc.* **93** (4), 485–498. <https://doi.org/10.1175/BAMS-D-11-00094.1>.
- Tran Anh, Q. & Taniguchi, K. 2018 Coupling dynamical and statistical downscaling for high-resolution rainfall forecasting: case study of the Red River Delta, Vietnam. *Prog. Earth Planet Sci.* **5**, 28. <https://doi.org/10.1186/s40645-018-0185-6>.
- Trinh-Tuan, L., Matsumoto, J., Tangang, F. T., Juneng, L., Cruz, F., Narisma, G., Santisirisomboon, J., Phan-Van, T., Gunawan, D., Aldrian, E. & Ngo-Duc, T. 2019 Application of quantile mapping bias correction for mid-future precipitation projections over Vietnam. *SOLA* **15**, 1–6. <https://doi.org/10.2151/sola.2019-001>.
- van Vuuren, D. P., Edmonds, J., Kainuma, M., Riahi, K., Thomson, A., Hibbard, K., Hurtt, G. C., Kram, T., Krey, V., Lamarque, J. F., Masui, T., Meinshausen, M., Nakicenovic, N., Smith, S. J. & Rose, S. K. 2011 The representative concentration pathways: an overview. *Clim. Change* **109**, 5. <https://doi.org/10.1007/s10584-011-0148-z>.
- Widmann, M., Bretherton, C. S. & Salathé Jr, E. P. 2003 Statistical precipitation downscaling over the Northwestern United States using numerically simulated precipitation as a predictor. *J. Clim.* **16** (5), 799–816. [https://doi.org/10.1175/1520-0442\(2003\)016<799:SPDOTN>2.0.CO;2](https://doi.org/10.1175/1520-0442(2003)016<799:SPDOTN>2.0.CO;2).
- Willmott, C. J., Clinton, M. R. & William, D. P. 1985 Small-scale climate maps: a sensitivity analysis of some common assumptions associated with grid-point interpolation and contouring. *Am. Cartographer* **12** (1), 5–16. <https://doi.org/10.1559/152304085783914686>.
- Wood, A. W. 2002 Long-range experimental hydrologic forecasting for the eastern United States. *J. Geophys. Res.* **107** (D20), 4429. <https://doi.org/10.1029/2001JD000659>.

- Wood, A. W., Leung, L. R., Sridhar, V. & Lettenmaier, D. P. 2004 Hydrologic implications of dynamical and statistical approaches to downscaling climate model outputs. *Clim. Change* **62**, 189–216. <https://doi.org/10.1023/B:CLIM.0000013685.99609.9e>.
- Wu, T. & Li, Y. 2013 Spatial interpolation of temperature in the United States using residual kriging. *Appl. Geogr.* **44**, 112–120. <https://doi.org/10.1016/j.apgeog.2013.07.012>.
- Xu, L. & Wang, A. 2019 Application of the bias correction and spatial downscaling algorithm on the temperature extremes from CMIP5 multimodel ensembles in China. *Earth Space Sci.* **6**, 2508–2524. <https://doi.org/10.1029/2019EA000995>.
- Zhang, Q., Shen, Z., Xu, C. Y., Sun, P., Hu, P. & He, C. 2019 A new statistical downscaling approach for global evaluation of the CMIP5 precipitation outputs: model development and application. *Sci. Total Environ.* **690**, 1048–1067. <https://doi.org/10.1016/j.scitotenv.2019.06.310>.

First received 9 April 2022; accepted in revised form 20 July 2022. Available online 6 August 2022